Impact of Fan Position and Speed Adjustments in Glass Greenhouse Environments

Junjie Huang *, #, Yingxiong Du #

School of Rail Transportation, Southwest Jiaotong University Hope College, Chengdu, China, 610400

* Corresponding author: JunjieHuang_stu@163.com

#These authors contributed equally.

Abstract. In the context of the contemporary development of precision agriculture, glass greenhouses, as an important infrastructure for enhancing crop production efficiency and quality, have become a frontier area of agricultural science and technology innovation for the internal microenvironmental regulation, especially the optimization of airflow dynamics and temperature distribution. In this paper, the study is based on the three-dimensional turbulence model equations of Reynolds number and Darcy-Forkheimer law, and modeled the cases without and with crops, simulated their different wind velocity and temperature, generated the corresponding simulation diagrams and analyzed them, and the results show that changing the Wind velocity to 3m/s or changing the fan position to 1m is a better condition than that with Wind velocity of 2m/s and fan position of 1.3m. In this study, it was found that both variables, Wind velocity and fan position, could affect the growth of crops in glasshouse, excluding most of the factors.

Keywords: glass greenhouse, CFD, Fluent, temperature simulation, wind speed simulation.

1. Introduction

With the advancement of science and technology, glass greenhouses play a vital role in growing vegetables in many areas of China in the opposite season. Appropriate temperature and wind speed are the key to plant growth, regulating the ventilation system to achieve the appropriate wind speed and temperature for crop growth in the greenhouse, greatly improves crop yield, quality, and economic benefits [1]. This paper establishes a physical model and a mathematical model of the influence of fan position and speed adjustment in a glass greenhouse and applies the κ-ε turbulence model, unstructured mesh, and finite volume method to numerical simulation calculations of the airflow field with and without crops and temperature field in a glass greenhouse [1]. The results of the study provide a useful reference for the research on the optimization of the position of the greenhouse fan and the speed of the warm air outlet in glass greenhouses. The research data for this article were obtained from the website (https://www.saikr.com/vse/apmcm/2023)

2. Airflow and Temperature Modeling for Crop-Free Greenhouses

2.1. Model Analysis

The main forms of energy exchange throughout the greenhouse are heat convection and heat conduction. One of the definitions of heat conduction is the phenomenon that occurs when substances have different internal temperatures, or when objects with different temperatures are in direct contact without relative displacement. Thermal convection is defined as the process by which heat energy is transferred between objects. The process does not require the transfer of matter but rather uses the temperature difference (the difference in temperature of the objects) as the driving force to transfer heat energy from the object with the higher temperature to the object with the lower temperature [1-2].

In this paper, we are based on a given glass greenhouse design with dimensions 10m×3m×2m (L×W×H) and a greenhouse fan with dimensions 0.5m×0.5m located on the left side of the greenhouse. The center of the greenhouse fan is 1.3 m above the ground and is simulated numerically using Fluent software. The control differential equations were discretized using the finite volume method and the SIMPLE algorithm was applied to solve the discrete control equations iteratively until convergence.

2.2. Modeling Steps

Using the Reynolds number three-dimensional turbulence model equation, Eq [3]. To simplify the problem, without taking into account the greenhouse door, airflow, solar radiation, and other external factors, the mathematical model of heat transfer by airflow inside the greenhouse can be described in tensor form as follows [4-5].

(1) Continuity equation

$$\frac{\partial u_i}{\partial x_i} = 0 \tag{1}$$

(2) Dynamic equations

$$\frac{\partial}{\partial x_i}\left(\rho_{n_i} u_j\right) = -\frac{\partial}{\partial x_T}\left(p + \frac{2}{3}\rho_k\right) + \frac{\partial}{\partial x_i}(\mu + \mu_t)\left(\frac{\partial u_i}{\partial x_j} + \frac{\partial u_j}{\partial x_i}\right) + \beta(T_0 - T)\rho_g] \tag{2}$$

(3) Turbulent energy equation

$$\frac{\partial}{\partial x_i}\left(\rho_{u_i} T\right) = \frac{\partial}{\partial x_i}\left(\frac{\mu}{pr} + \frac{\mu_t}{\sigma^T}\right)\frac{\partial T}{\partial x_i} + \frac{q}{C_p} \tag{3}$$

(4) Turbulent pulsation kinetic energy equation

$$\frac{\partial}{\partial x_i}(\rho u_i T) = \frac{\partial}{\partial x_i}\left(\frac{\mu}{\sigma_k}\frac{\partial k}{\partial x_i}\right) + G - \rho_\varepsilon + \beta g \frac{\mu_t}{Pr}\frac{\partial T}{\partial x_i} \tag{4}$$

(5) Turbulent pulsation kinetic energy dissipation rate equation

$$\frac{\partial}{\partial x_i}\left(p_{u_i}\varepsilon\right) = \frac{\partial}{\partial x_i}\left[\left(\mu + \frac{\mu_t}{\sigma_\varepsilon}\right)\frac{\partial \varepsilon}{\partial x_i}\right] + (c_1 G - c_2 \rho\varepsilon)\frac{\varepsilon}{k} \tag{5}$$

The turbulent pulsation kinetic energy generation term in the equation is equated as follows.

$$G = \mu_t\left(\frac{\partial u_i}{\partial x_j} + \frac{\partial u_j}{\partial x_i}\right)\frac{\partial u_i}{\partial x_j} \tag{6}$$

Turbulent viscosity coefficient expression:

$$\mu_t = \frac{c_\mu \rho k^2}{\varepsilon} \tag{7}$$

In these equations, $c_1, c_2, c_\mu, \sigma_k, \sigma_{\varepsilon,}\sigma_T$ are empirical constant; C_p is Constant-pressure specific heat of air $(kJ/(kg \cdot K))$;g is the acceleration of gravity(m^2/s); k is fluid turbulence pulsation kinetic energy (m^2/s);p is average hourly pressure(pa); P_r is Prandtl number during turbulence; q is intensity of thermal source (W/m^3); T is fluid temperature(K); T_0 is reference temperature (K); $u_i$is component of velocity(m/s); direction of the $\mathrm{x}-$axis:$\mathrm{i} = 1$; direction of the $\mathrm{y}-$axis; $\mathrm{i} = 2$; direction of the $\mathrm{z}-$axis: $\mathrm{i} = 3$; ε is turbulent energy dissipation rate $(m^2 \cdot s)$; μ is Coefficient of kinetic viscosity(m^2/s);μ_t is coefficient of viscosity of turbulent flow dynamics(m^2/s); ρ is fluid density(kg/m^3);β is Fluid volume expansion coefficient $(1/K)$.

2.3. Meshing Details

For the outdoor space of the hexahedral structure greenhouse, the greenhouse fan is set as the velocity inlet boundary condition with a wind speed of 2 m/s, while the top and perimeter of the greenhouse as well as the ground are treated with the walls as the boundary condition. The specific parameter settings are shown in Table 1.

The roof of the glasshouse is distributed in a rectangular shape, and an unstructured mesh is chosen to discretize the whole glasshouse. Considering the complex flow conditions at the outlet of the greenhouse fan, the mesh in this region is appropriately encrypted [6]. The overall mesh of the greenhouse is shown in Fig. 1, with 11, 045 nodes and 54, 230 individual meshes. The maximum mesh deformation rate is 0.79, and the mesh quality is good, which meets the requirements of the subsequent simulation.

Table 1. Basic parameters and boundary conditions

Parameters	Numerical value
air density/$(\mathrm{kg\cdot m^{-3}})$	1.225
Thermal conductivity of air/$(\mathrm{W\cdot m^{-1}\cdot K^{-1}})$	0.0225
Coefficient of thermal expansion of air/$\mathrm{K^{-1}}$	3.356×10^{-3}
Specific heat capacity of air/$(\mathrm{J\cdot kg^{-1}\cdot K^{-1}})$	1005
aerodynamic viscosity/$(\mathrm{kg\cdot m^{-1}\cdot s^{-1}})$	1.83×10^{-5}
Glass density/$(\mathrm{kg\cdot m^{-3}})$	2500
Thermal conductivity of glass/$(\mathrm{W\cdot m^{-2}\cdot K^{-1}})$	0.74
convective heat transfer coefficient/$(\mathrm{W\cdot m^{-2}\cdot K^{-1}})$	6..6
Fan speed/$(\mathrm{m\cdot s^{-1}})$	5.0
Fan outlet temperature/℃	40
environmental temperature/℃	33
ground temperature/℃	28
Crop canopy pressure drop coefficient$(\mathrm{C_0})$	0.395
Internal loss factor$(\mathrm{C_1})$	0.2
Crop porosity	0.7

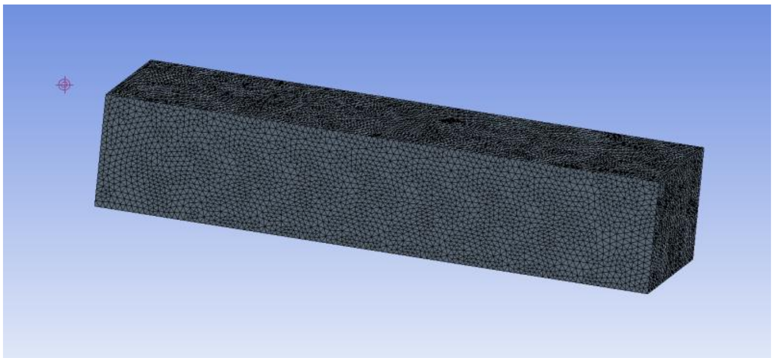

Figure 1. Mesh generated in the greenhouse calculation domain

2.4. Numerical Simulation

Fluent is used for numerical simulations. The finite volume method is used for discrete control differential equations and SIMPLE algorithm is used to solve discrete control equations. The convective terms are in windward differential format [7]. At the beginning of the iteration, the relaxation factor is halved to simulate 100 iterations with the laminar flow model. After the flow field develops smoothly, the default relaxation factor is restored, the numerical model is recovered as a κ-ε turbulence model, and the mesh is refined according to the velocity gradient, after which the number of mesh cells is increased to 573, 729, and then the computation is continued iteratively until convergence [8].

2.5. Simulated Results

This simulation iteration uses an adaptive step size and stabilizes after approximately 800-time steps. The results of the computational simulation are shown in Fig. 2.

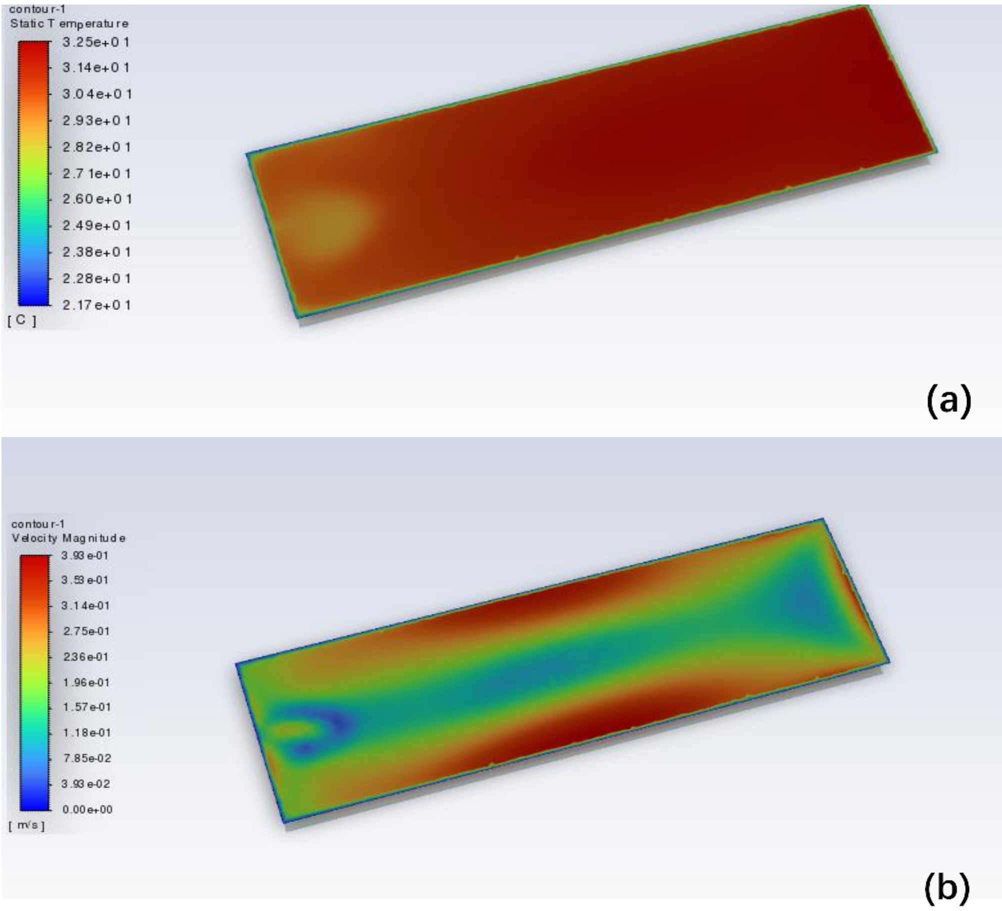

Figure 2. Simulated distribution of z=0.5 cross-section of crop-free greenhouse (a) temperature (b) wind velocity

3. Crop-Containing Greenhouse Climate Simulations

3.1. Model Analysis

We base our study on an indoor glass greenhouse with a design specification of 10m×3m×2m (L×W×H), and a greenhouse fan with a size of 0.5m×0.5m, located on the left side of the greenhouse. The center of the greenhouse fan is located at 1.3m above the ground, and the steady state simulation of the flow field is performed based on the full size of the greenhouse, in the simulation analysis, it is known that the cropping model is a porous medium, and the crop model is simplified to a specification of 8m×2m×0.5m (L×W×H), and the location is located in the center of the greenhouse.

3.2. Modeling

Crops grown in greenhouses in the simulation were analyzed by simplifying the cropping model to a porous medium. According to the modeling of the greenhouse without crops, a pressure drop occurs when the airflow flows through the porous medium. This process can be described by Darcy's equation [8]:

$$-\frac{\partial p}{\partial x_i} = \frac{\mu}{K_L} U_i + K_{loss}\rho|U|U_i \quad (8)$$

Terrestrial evaporative fluxes:

$$M_s = \frac{|x_s - x_i|}{r_s} \quad (9)$$

In the equation, M_s is the evaporation flux from the soil, $\mathrm{kg/(m^2 \cdot s)}$; x_s, x_i represents the absolute humidity of the soil and indoor air, kg/m^3.c is the soil boundary layer resistance,s/m, also the following formula:

$$r_s = \frac{1}{\kappa^2 u(z)}\left[\ln\left(\frac{z+z_0}{z_0}\right)\right]^2 \tag{10}$$

In the equation, κ is the Kamen number, which has a value of 0.41;u(z) is the wind speed at a height of meters from the ground,m/s; and z_0 is the roughness length, m, which takes the value of 0.1 on a level soil surface.

The evaporation flux from the soil was converted in the simulation to volumetric evaporation on each computational grid according to the volume of soil occupied in the cultivation tank [8].

In addition, the sensible heat exchange between the crop canopy and the air inside the temperature chamber and the latent heat of transpiration of the crop is calculated according to the following equations and added to the energy approach as source terms. The first part on the right side of the equation is the sensible heat and the second part is the latent heat [9]:

$$S_\phi = 2LAI\rho C_\rho \frac{T_c - T_i}{r_a} + LAI\rho\lambda \frac{H_c - H_a}{r_a + r_s} \tag{11}$$

In the equation, S_ϕ is the source term of the energy equation; LAI is the leaf area index, m^2/m^2; T_c and $T_i$are the crop as well as indoor air temperatures, K; r_a is the aerodynamic obstruction in the crop boundary layer,s/m; and H_c and H_a are the relative humidity of the crop and indoor air, respectively.

3.3. Meshing

The roof of the glasshouse is distributed in a rectangular shape and an unstructured mesh is chosen to discretize the whole glasshouse. Considering the complex flow conditions at the outlet of the greenhouse fan, the mesh was appropriately encrypted. There are 52,296 nodes and 217,930 individual meshes. After checking, the maximum mesh distortion rate is 0.8, and the mesh quality is good, which meets the requirements of subsequent simulations.

3.4. Numerical Simulation

Fluent is used for numerical simulations. The finite volume method is used for discrete control differential equations and SIMPLE algorithm is used to solve discrete control equations. The convective terms are in windward differential format. At the beginning of the iteration, the relaxation factor is halved and 100 iterations are simulated with a laminar flow model. After the flow field develops smoothly, the default relaxation factor is restored, the numerical model is reverted to a κ-ε turbulence model, and the mesh is refined according to the velocity gradient, after which the number of mesh cells is increased to 436731, and then the computation is continued iteratively until convergence [8].

3.5. Simulated Results

This simulation iteration uses an adaptive step size and stabilizes after approximately 800-time steps. The results of the computational simulation are shown in Fig.3 and Fig.4.

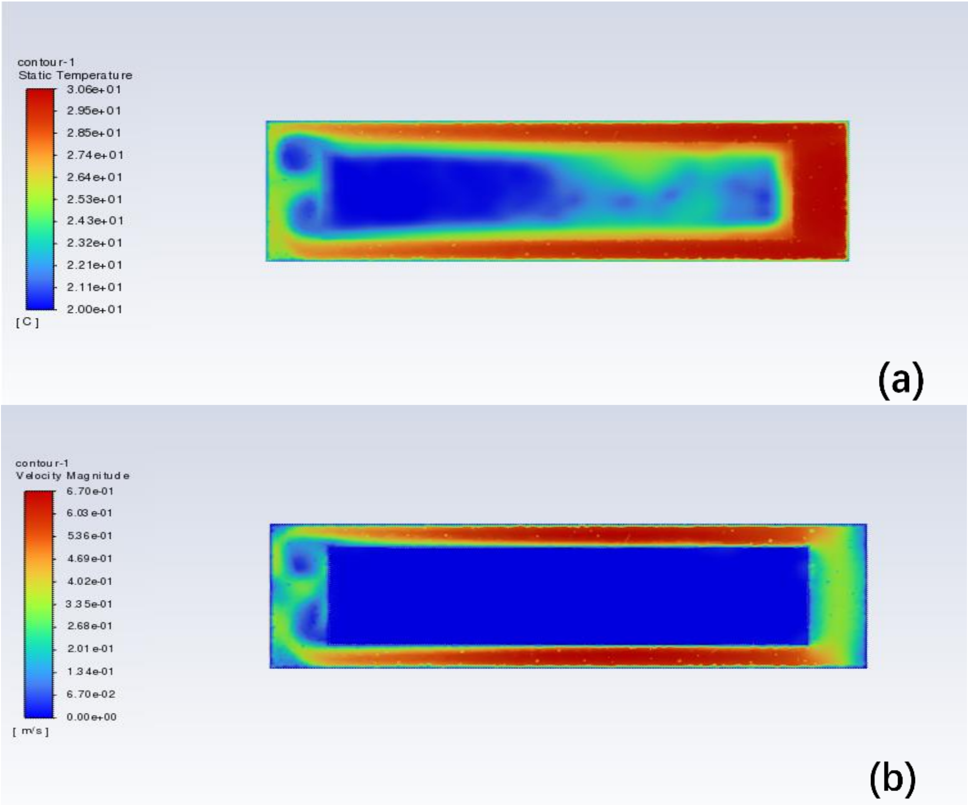

Figure 3. Simulated distribution of z=0.1 cross-section of crop-containing greenhouse (a) Temperature (b) Wind velocity

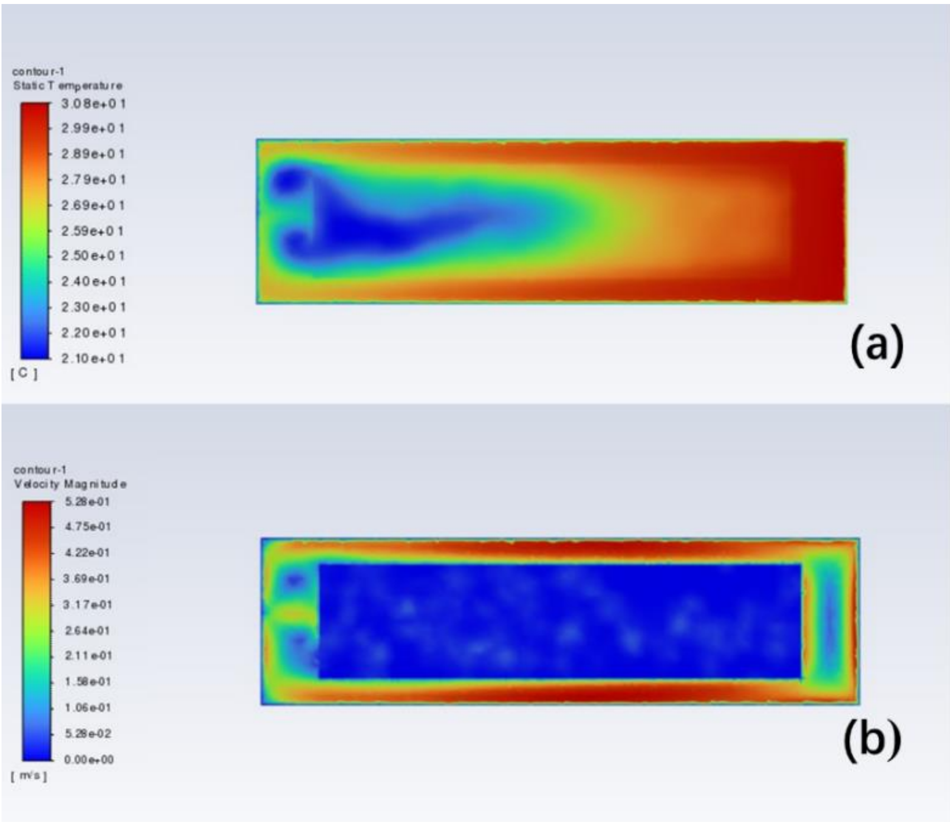

Figure 4. Simulated distribution of z=0.5 cross-section of crop-containing greenhouse (a) Temperature (b) Wind velocity

4. Optimizing greenhouse Fan Design

To simplify the problem of optimizing the greenhouse fan design, only the fan speed and fan position are changed in this paper.

In Scenario 1, the simulation program changed the wind speed to 3m/s; in Scenario 2, the simulation program changed the fan location to 1m. CFD simulations and analysis were performed. Comparisons were made with Figures 3 and 4, thus qualitatively determining that greenhouse systems with different wind speeds and different fan positions are more beneficial to crop growth in a reasonable configuration.

This simulation iteration uses an adaptive step size and stabilizes after approximately 800-time steps. The results of the computational simulation for Scenario 1 are shown in Fig. 5 and Fig. 6, and the results of the computational simulation for Scenario 2 are shown in Fig. 7 and Fig. 8.

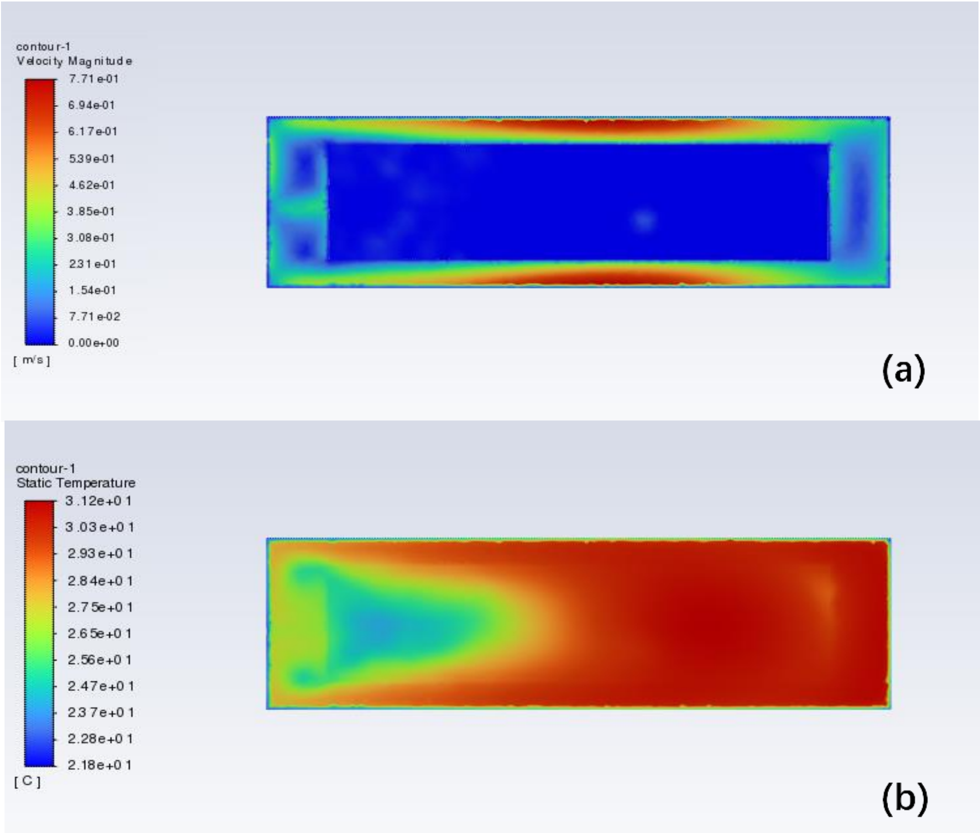

Figure 5. Simulated distribution of crop-containing greenhouses at a wind velocity of 3 m/s, z=0.1 cross-section (a) Wind velocity (b) Temperature

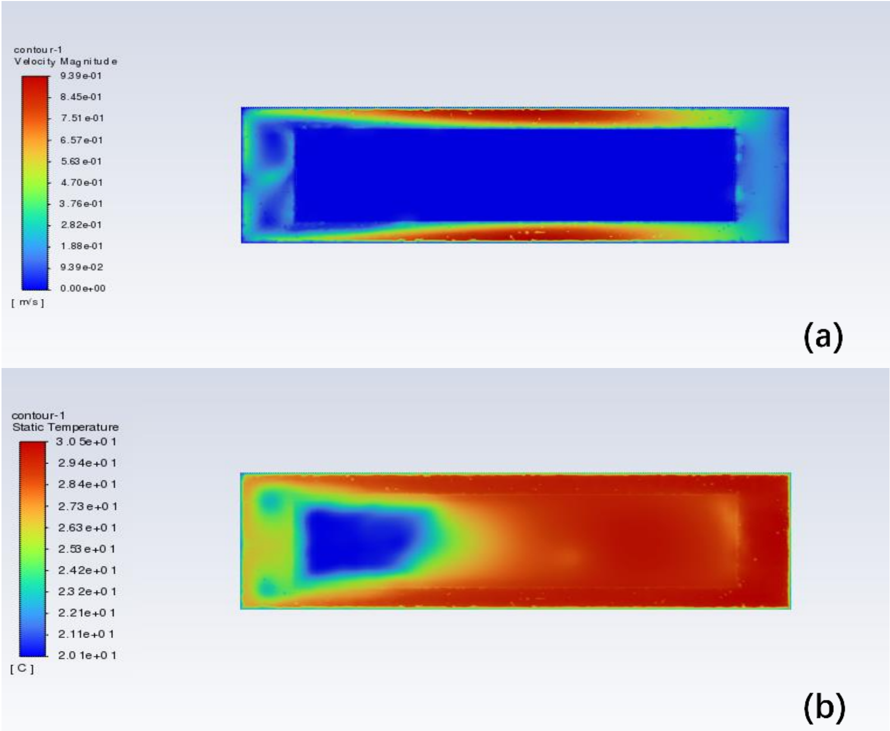

Figure 6. Simulated distribution of crop-containing greenhouse at wind velocity of 3 m/s,z=0.5 cross-section (a) Wind velocity (b) Temperature

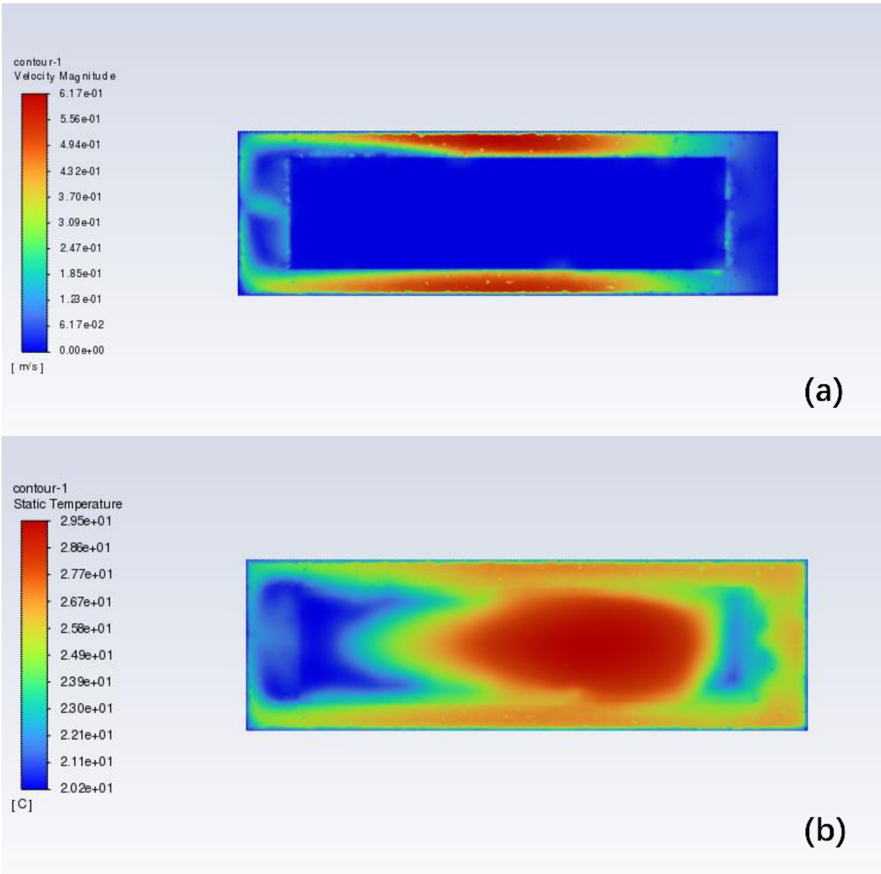

Figure 7. Cross-sectional distribution of crop-containing greenhouse at fan position 1m, z=0.1 (a) Wind velocity (b) Temperature

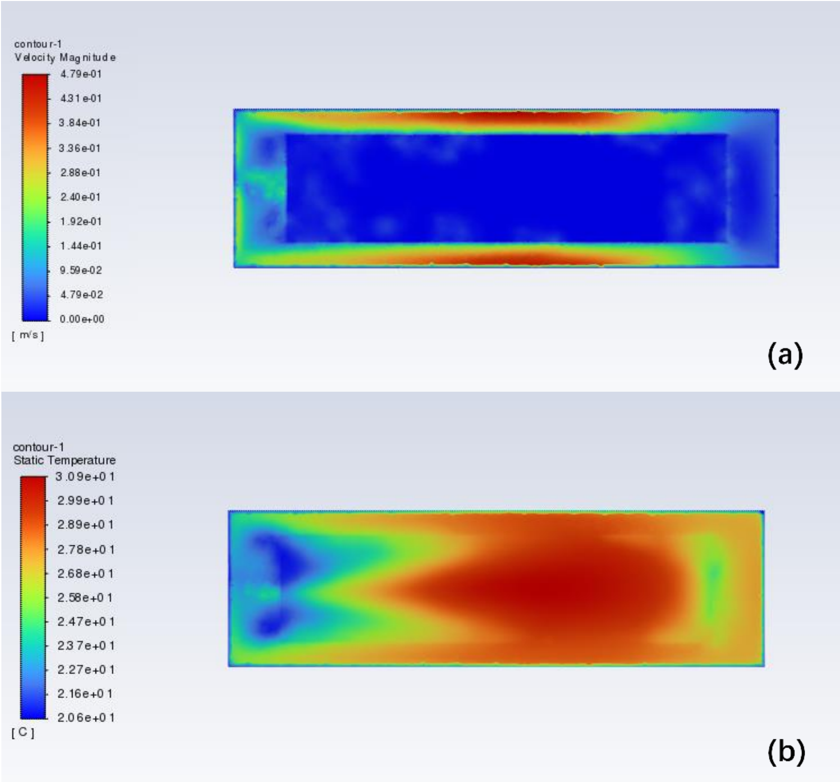

Figure 8. Simulated distribution of crop-containing greenhouse at fan height of 1m, z=0.5 cross-section (a) Wind velocity (b) Temperature

5. Conclusion

The study in this paper is based on the analysis of crop-free greenhouse simulation maps and crop-containing greenhouse simulation maps for different scenarios:

From the cloud map of the crop canopy, it can be seen that in the region of the greenhouse away from the fan, various vortices are formed due to the greenhouse boundary, crop constraints, and air resistance of the crop [10] and the complexity of the airflow creates a higher Wind velocity. The cloud map of airflow distribution within the crop canopy shows that even the complexity of the canopy airflow has minimal effect on the airflow within the canopy.

As can be seen from the temperature distribution cloud diagram, the temperature at different heights still has obvious differences. Considering only the case of Wind velocity, the larger the value of its wind velocity, the better the cooling effect of the greenhouse; the temperature distribution cloud map of the crop canopy may appear in a small part of the area if the temperature is low, this height is mostly close to the location of the fan outlet [11], but in the case of increased Wind velocity, the cooling effect of the greenhouse has also been strengthened, and the occurrence of low temperatures is a normal phenomenon, and the closer the area of the fan outlet about the more likely to appear low temperatures, but also A small portion of the crop showed low temperatures, while the overall crop was not affected. In the cases simulated for the existing conditions, the conditions for crop growth were better than those with a Wind velocity of 2 m/s and a fan position of 1.3 m, both when the Wind velocity was changed to 3 m/s and when the fan position was changed to 1m.

References

[1] WU Feiqing, XU Fang, ZHANG Libin, et al. Numerical simulation of the heating environment of glass greenhouse based on porous medium [J]. Journal of Agricultural Machinery, 2011, 42 (02): 180 - 185.

[2] ZHANG Qi-Xun, YU Hai-Ye, ZHANG Zhong-Yuan et al. Study of airflow in a solar greenhouse using CFD model [J]. Journal of Agricultural Engineering, 2012, 28 (16): 166 - 171.

[3] WANG Zaihong, TAO Haichen, XU Wei et al. Cultivation technology of cherry tomato in a glasshouse in Shanghai [J]. Shanghai Vegetable, 2023, (01): 33 - 34.

[4] YE Chao, YAO Wenbin, WAN Hang. Temperature control of small flower glass greenhouse based on PLC fuzzy control [J]. Science and Technology Perspectives, 2021, (10): 36 - 38.

[5] JIN Jing. Analysis of soilless cultivation technology of tomato in glass greenhouse [J]. Modern Horticulture, 2019, (08): 17 - 18.

[6] ZHAO Na, LI Ming, ZHAO Shumei et al. CFD simulation of the effect of ducted air supply system on airflow and temperature fields in plastic greenhouses [J]. Journal of China Agricultural University, 2023, 28 (08): 272 - 281.

[7] LI Xiaqing, DENG Shuhui, RU Lin et al. Simulation analysis of winter greenhouse based on CFD [J]. Modernized Agriculture, 2023, (02): 82 - 85.

[8] LIU Liansheng, MENG Guo, WANG Dongji et al. Simulation study of daylight greenhouse environment under different thermal insulation and heating conditions based on CFD [J]. Journal of Shenyang Agricultural University, 2022, 53 (06): 709 - 716.

[9] Gao Lijun, Tana, Jiao Wei et al. Characterization and numerical simulation of temperature and humidity distribution in sub-canopy surface soil of solar greenhouse crops [J]. Journal of Inner Mongolia Agricultural University (Natural Science Edition), 2022, 43 (04): 4956.

[10] WANG Yingyi, ZHANG Xu, DENG Xin, et al. Numerical simulation analysis of greenhouse based on computational fluid dynamics [J]. Science and Technology Innovation, 2021, (01): 21 - 22.

[11] YIN Kuichao. CFD simulation analysis of natural ventilation in a greenhouse [J]. Building Thermal Ventilation and Air Conditioning, 2020, 39 (04): 88 - 91.